Capacity-Aware Undersea Cable System Design

Tianjiao Wang, Bill Moran, Moshe Zukerman, *Life Fellow, IEEE*

***Abstract*—Undersea cables play a crucial role in enabling global communication and data transfer, significantly affecting Internet speeds. Without them, global communication would be severely limited. As technology advances and network demands increase, the number and variety of optical fibers within cables are constantly increasing. This growth results in more costly cable networks with the ability to transmit more data and enhances the speed and reliability of data transmission. The construction of an undersea cable system requires careful consideration of the appropriate bandwidth of the cable to meet network bandwidth requirements while minimizing costs. In this paper, we formulate the undersea cable network optimization problem taking account of the bandwidth capacity of each cable edge on the cable network as a weighted edges Steiner minimum tree problem and describe a new algorithm called the *weighted edges* Steiner minimum tree (WE-SMT) algorithm. For the given locations of the terminal nodes and the bandwidth capacity requirement, the WE-SMT algorithm optimizes the position of Steiner nodes, the bandwidth capacity of each cable edge, and the cable path. We implement our algorithm in a real-world setting, evaluating the benefit gained against the outcomes obtained without accounting for bandwidth optimization, as well as studying the effect of data resolution on the quality of the path planning results. In addition, we assess the performance of our new algorithm in comparison with that of an operational real-world cable system.**

***Index Terms*—Cable network, bandwidth, capacity, Steiner minimum tree**

I. Introduction

While satellite links can provide inter-continental communication, it is overwhelmingly done through fiber optic undersea cables on the seabed. According to [1], undersea optical internet cables play a crucial and important role in global communication, transmitting over 99% of global internet data. Specialized ships deploy optical undersea cables, connecting terminal stations located on the shores [2]. Cables accommodate multiple fibers, each with a high bandwidth capacity, allowing faster and more efficient data transfer [3, 4] than satellites. In part, this is because undersea cables are more cost-effective for long-term, high-volume communication, though the costs of these cables usually increase with the number of optical fibers [5]. Undersea cable costs are also influenced by seabed topography, ocean environment, and communication demands [6].

Typically, newer cables carry more data than cables laid 15 years ago: increasing from hundreds of megabits per second to hundreds of terabits per second (Tb/s) capacity currently [7, 8]. For example, the new MAREA cable can carry 224 Tb/s. The highest capacity undersea cable currently in operation is Google Cloud's trans-Atlantic system, Dunant, with a capacity of 250 Tb/s across 12 fiber pairs, and spanning 4.1k miles (6.6k kilometers), connecting Virginia Beach (United States) with Saint-Hilaire (France) [8]. Historically, undersea cables were built with 4 to 8 fiber pairs, but new ocean internet cables are being built with 12, 16, 24, and 36 fiber pairs [8]. In densely populated and economically developed areas, there is a higher demand for communication efficiency and quality [9]. More optical fibers mean greater transmission capacity and bandwidth. This enables support for more data transmission and higher communication speeds, meeting the growing demands of the network [10].

To optimize a cable network, it is essential to minimize the total cost of all components while maintaining the quality of service (QoS) requirements. This involves optimizing the location of (branching units) BUs and (cable landing stations) CLSs, calculating the cable path based on geodesics, and taking into account the bandwidth requirements of the cable. Previous publications on cable network design, e.g. [11–13] and references therein, have addressed all the above-mentioned aspects except for the consideration of cable bandwidth requirements.

In this paper, we formulate the undersea cable network optimization problem as a weighted edges Steiner minimum tree problem. To obtain the weighted cost between pair of nodes, we employ the fast marching method (FMM) which was used for point-to-point cable path planning in [11–15]. However, unlike the previous use of FMM for point-to-point cost calculations, here we take into account the cost associated with the bandwidth capacity. We use this FMM-based approach to obtain the cost of each edge in the network. This is an important consideration for optimizing undersea cable networks. We propose the weighted edges Steiner minimum tree (WE-SMT) algorithm to effectively optimize the position of Steiner nodes, the bandwidth capacity of each

This work was supported by the Hong Kong Innovation and Technology Commission (InnoHK Project CIMDA), and by a grant from the Research Grants Council of the Hong Kong Special Administrative Region, China (CityU 11201922). *(Corresponding author: Tianjiao Wang)*

Tianjiao Wang is with the Center for Intelligent Multidimensional Data Analysis, Hong Kong Science Park, Shatin, Hong Kong. A significant part of this work was done when Tianjiao Wang was with the Department of Electrical Engineering, City University of Hong Kong, Kowloon, Hong Kong SAR, China (e-mail: tianjwang6-c@my.cityu.edu.hk).

Moshe Zukerman is with the Department of Electrical Engineering, City University of Hong Kong, Kowloon, Hong Kong SAR, China (e-mail: m.zu@cityu.edu.hk).

Bill Moran is with the Department of Electrical and Electronic Engineering, The University of Melbourne, Melbourne, VIC 3010, Australia (e-mail: wmoran@unimelb.edu.au).

cable edge, and the cable path for given terminal node locations and bandwidth capacity requirements. Our new WE-SMT algorithm can be applied to real-world scenarios, making it a practical solution for optimizing undersea cable networks.

We conduct a comparative analysis between our bandwidth-optimized results and those obtained from a design based on [12], which did not incorporate bandwidth optimization. In the latter design, cable capacity is held constant to meet bandwidth requirements. This comparison is done to provide quantitative value to cost savings achieved by the added component of bandwidth optimization. Furthermore, we extend our comparison to an existing cable system, Medloop, as documented in [1]. It is essential to acknowledge that when comparing with an existing cable system, the original designer might have had access to proprietary data that is not available to us. Any conclusions about comparison must be made keeping this fact in mind. In addition, we have thoroughly studied the effect of data resolution on path planning results and cost optimization. As mentioned in [11–15], the FMM-based algorithm is optimal given the data, and it is expected that higher data resolution will improve the optimal path planning results.

The remainder of this paper is organized as follows. In Section II, we briefly review related path planning research in cable networks involving capacity considerations. Section III focuses on the modeling of our cable network optimization accommodating the bandwidth requirement problem. In Section IV, we propose the WE-SMT method to solve the problem. The performance of our method is demonstrated by several numerical simulations based on realistic examples in Section V. Finally, we conclude the paper in Section VI.

II. Related Work

Currently, within the general area of undersea cable path optimization, it is reasonable to delineate several sub-areas, and we go through these here.

Firstly, for existing research on point-to-point cable path planning research, we discuss [14–16]. In [14], Wang *et al.* presented a method based on the FMM for cable path planning on the earth's surface. FMM is an optimal approach for point-to-point path planning, as it solves the Eikonal equation when the grid size of the triangulated manifold tends to zero [17]. Wang *et al.* addressed the cable path planning problem as a multi-objective optimization problem, taking into account cable breaking risk, cable laying cost, and multiple design levels for cable shielding. This work was used in [15] to demonstrate that the FMM-based approach can achieve automatic cable path planning which is close to a real-life cable that was designed manually by a team of planners and surveyors.

Blaise *et al.* [16] proposed a Dijkstra-based method to determine the cable path with minimal cost involving constraints on the cable path planning process to avoid undesirable regions. In addition, the numerical solver based on their method was implemented on parallel architectures, which can provide optimal paths of real-life examples in acceptable computational times. The drawback of the Dijkstra-based method is that the path must traverse either a diagonal or lateral edge between adjacent cells, which makes the result inferior to that of FMM as shown in [17]. In addition, parallel computing of FMM as in [18] can also be used to reduce runtime if necessary. Parallel processing solutions for cable path planning are available for both FMM [18] and DA [16]. None of the aforementioned publications addressed the key consideration of bandwidth optimization.

For cable network design problems, Wang *et al.* [11] proposed a method based on FMM and Integer Linear Programming to optimize a tree-topology network design for an undersea cable system that connects multiple stations. Additionally, the authors proposed a lightweight heuristic algorithm to solve the problem at hand. The optimization problem was formulated as a minimum spanning tree (MST) problem, where the goal was to construct a tree-topology cable network without additional Steiner nodes at minimum cost.

Wang *et al.* [19] proposed an FMM-based method to achieve a trunk-and-branch tree network topology for undersea cable systems that connect multiple landing stations. That work considered the optimization of the trunk-and-branch tree network problem as a Steiner minimum tree (SMT) problem and, based on dynamic programming, obtained the minimum tree on an irregular 2-dimensional manifold in a 3-dimensional Euclidean space for a given topology in polynomial time. The construction of minimum spanning trees on such a manifold is the innovation in the work of Wang *et al.*. This is a departure from traditional research on minimum Steiner trees, such as [20, 21], primarily focused on discussions in Euclidean spaces. The studies referenced above solely focus on cable construction costs, neglecting the expenses associated with bandwidth requirements and Branching Unit (BU) installation. We incorporated the BU and cable landing station costs into an analysis of the total network cost in [12]. As in [19], we have regarded the cable network as an SMT problem with the addition of the weighted BU. The algorithm proposed in [12] can also be applied to area connection optimization. However, the issues and expenses associated with the bandwidth requirements have not been taken into account in the previous work on cable network optimization, and these are the foci and the novel aspects of this paper.

Next, we briefly discuss papers that take account of capacity considerations in the context of individual cables and not of cable networks. Downie *et al.* [22] discussed the comparison of capacity and cost/capacity between 4-core fibers and single-core fibers in undersea cables. They evaluated these two types of fibers using mathematical models and experimental data and compared their technical characteristics, costs, and per-

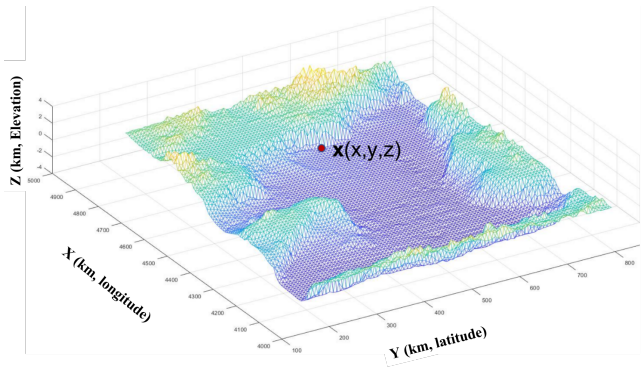

Fig. 1: The model of the earth's surface.

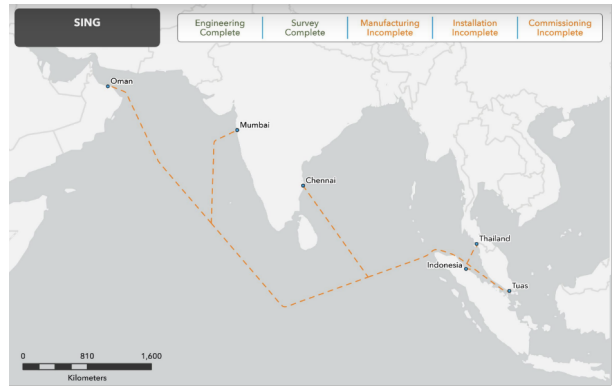

Fig. 2: A Real-World Cable Network (SING) with Trunk-and-Branch Tree Topology [1].

formance. The study in [23] analyzes the maximum cable capacity achievable with multi-core fibers with different core counts and compares it to single-core fiber systems. The research takes into account factors like power limitations, crosstalk between cores, and the cost-effectiveness of multi-core fiber systems. Their research was intended to provide decision support for decision-makers, designers, and operators in choosing fibers for undersea cable systems. It is important to note that their study focused on cable capacity comparison rather than cable path optimization.

III. Problem Modeling and Description

As in [15, 19], to well-approximate the earth's surface, we use a triangulated piecewise-linear 2D manifold $\mathbb{M}$ in 3D space, as illustrated in Fig. 1. A coordinate system is defined on the seabed surface which helps in the location of objects and geographical features. Each grid node $\mathbf{x}$ on $\mathbb{M}$ is represented by 3D coordinates (x, y, z), where $z = \xi(x, y)$ is the altitude of the geographic location (x, y). This approach is different from the usual approaches to network design where the entire network is in Euclidean space, e.g. [24–26].

Our objective is to establish a trunk-and-branch tree topology cable network to ensure that capacity demand requirements between specified nodes are met at the lowest possible cost. The cost aspect will be discussed in detail later. Fig. 2 shows a real-world cable network with a trunk-and-branch tree topology that includes five terminals and three BUs. The edges of the SMT are computed to be minimal-cost cable paths in $\mathbb{M}$. This is different from the common practice of using software to produce routes based on great circles [27]. In $\mathbb{M}$, paths of cables between pairs of terminals, or Steiner nodes, are geodesics relative to the cost function and are calculated using the FMM [14]. Optimal connections between nodes are shaped according to localised costs of the specific path.

To be a little more precise, $\mathbf{M}$ is defined to be the set of mesh points in the compact triangulated $\mathbb{M}$; N is the number of terminal nodes, $\mathbf{B}$ is the set of capacity requirement between pairs of terminal nodes; N_b is the number of Steiner nodes; $\mathbf{S} = \{\mathbf{s}_1, \mathbf{s}_2, \ldots, \mathbf{s}_{N_b}\}$ is the set of their locations; $\mathbf{\Gamma}$ is the set of geodesics of the Steiner tree; c_b is the cost of a BU (all BUs have the same cost in our model); l_i is an edge of the Steiner tree; b_i is the bandwidth of the corresponding edge l_i; $p(\mathbf{x}_i, \mathbf{x}_j)$ is the path between nodes $\mathbf{x}_i$ and $\mathbf{x}_j$, which may includes several edges; $Br(\mathbf{x}_i, \mathbf{x}_j)$ is the bandwidth requirement of path $p(\mathbf{x}_i, \mathbf{x}_j)$. We write $f(\mathbf{s})$ for the cost of the cable system; this depends on the cost of BUs and cable links, as shown in Eq. (1). The cost of cable links depends on the capacity of the cable and the cable length.

Table I provides descriptions for notations used in this paper.

Table of Notations	
$\mathbb{D}$	the objective region
$\mathbb{M}$	triangulated manifold in $\mathbb{R}^3$
(x, y, z)	coordinate of a point in $\mathbb{M}$
$c(\mathbf{x})$	cost at location $\mathbf{x}$
e(i,j)	edge connects two nodes $\mathbf{x_i}$ and $\mathbf{x_j}$
b(e(i,j))	bandwidth of edge e(i,j)
$\mathbf{M}$	set of mesh points in $\mathbb{M}$
$\mathbf{s}_1, \mathbf{s}_2, \ldots, \mathbf{s}_{N_b}$	Steiner node
$\mathbf{S}$	set of the Steiner node locations
$\mathbf{\Gamma}$	set of geodesics of the Steiner tree
c_b	cost of a BU
l_i	link in the Steiner tree
b_i	bandwidth of the corresponding link l_i
$p(\mathbf{x}_i, \mathbf{x}_j)$	path between nodes $\mathbf{x}_i$ and $\mathbf{x}_j$
$Br(\mathbf{x}_i, \mathbf{x}_j)$	bandwidth requirement of path $p(\mathbf{x}_i, \mathbf{x}_j)$
$f(\mathbf{s})$	cost of the cable system

TABLE I

$$f(\mathbf{s}) = \sum_{\gamma_i \in \mathbf{\Gamma}} C(\gamma_i) + c_{BU} \cdot N_{BU}. \tag{1}$$

The cost $C(\gamma)$ of a cable along geodesic γ depends on several factors but, to a good approximation grows, as the geodesic length of the cable:

$$\mathrm{C}(\gamma) = \int_0^{l(\gamma)} c(\gamma(s), b) ds, \tag{2}$$

where the local cost $c(\gamma(s), b)$ at location s is a function of the laying cost in location $\gamma(s)$, risks associated with the locality, and b is the bandwidth of the cable.

The relationship between bandwidth and cable cost per kilometer is assumed to be $c(\mathbf{x}) = b \cdot \mathbf{x} + A$, where b is the bandwidth capacity of the cable, measured in the number of fibers. The fixed cost of cable construction, denoted by A, is determined by industry experts.

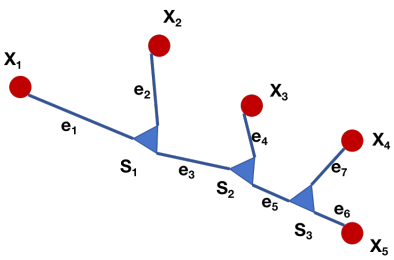

(a) The corresponding topology of Fig 2.

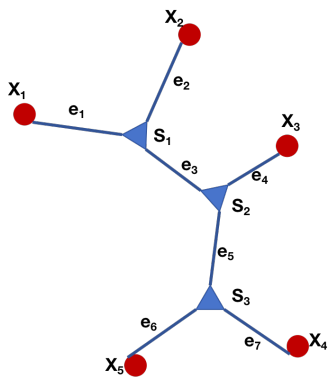

(b) The standardized topology.

Fig. 3: The topology for the cable network (SING).

The corresponding topology of the cable network in Fig. 2 is displayed in Fig. 3(a), which consists of five terminals, namely $\mathbf{x}_1$, $\mathbf{x}_2$, $\mathbf{x}_3$, $\mathbf{x}_4$, and $\mathbf{x}_5$, connected to three Steiner nodes (representing BUs) denoted by s_1, s_2 and s_3, along with five cable links represented by edges e_1, e_2, e_3, e_4, e_5, e_6, and e_7. In a tree topology network, there is only one path $p(\mathbf{x}_i, \mathbf{x}_j)$ connects each pair of nodes, $\mathbf{x}_i$ and $\mathbf{x}_j$; and $Br(\mathbf{x}_i, \mathbf{x}_j)$ is the bandwidth requirement. Each edge e_i should accommodate the bandwidth requirements of paths that include this edge, eg. edge e_1 has to accommodate the bandwidth requirements of paths $p(\mathbf{x}_1, \mathbf{x}_2)$, $p(\mathbf{x}_1, \mathbf{x}_3)$, $p(\mathbf{x}_1, \mathbf{x}_4)$, and $p(\mathbf{x}_1, \mathbf{x}_5)$, so that,

$$b(e_1) \geq Br(\mathbf{x}_1, \mathbf{x}_2) + Br(\mathbf{x}_1, \mathbf{x}_3) + Br(\mathbf{x}_1, \mathbf{x}_4) + Br(\mathbf{x}_1, \mathbf{x}_5).$$

Similarly, edges e_2 needs to handle the bandwidth requirements of paths $p(\mathbf{x}_1, \mathbf{x}_2)$, $p(\mathbf{x}_2, \mathbf{x}_3)$, $p(\mathbf{x}_2, \mathbf{x}_4)$, and $p(\mathbf{x}_2, \mathbf{x}_5)$.

Cable edge costs are determined by the number of fibers in, and the hence capacity of the cable. To minimize total costs, higher bandwidth edges need to be short. Minimization of the total cost of the cable system requires optimal placement of the three BUs, s_1, s_2 and s_3, and this involves factoring in the costs of the five cable edges, each with different bandwidth requirements and costs, as well as the cost of the BUs.

For this five terminal nodes example, taking into account the cable system optimization problem, the cable bandwidth capacity can be written as:

$$\begin{aligned}
\min_{\mathbf{SMT}} \; & S \in H, \mathbf{\Gamma} \quad f(\mathbf{s}) \\
\text{s.t.} \quad & b(e_1) \geq Br(\mathbf{x}_1, \mathbf{x}_2) + Br(\mathbf{x}_1, \mathbf{x}_3) + Br(\mathbf{x}_1, \mathbf{x}_4) + Br(\mathbf{x}_1, \mathbf{x}_5), \\
& b(e_2) \geq Br(\mathbf{x}_1, \mathbf{x}_2) + Br(\mathbf{x}_2, \mathbf{x}_3) + Br(\mathbf{x}_2, \mathbf{x}_4) + Br(\mathbf{x}_2, \mathbf{x}_5), \\
& b(e_3) \geq Br(\mathbf{x}_1, \mathbf{x}_3) + Br(\mathbf{x}_1, \mathbf{x}_4) + Br(\mathbf{x}_1, \mathbf{x}_5) \\
& \qquad + Br(\mathbf{x}_2, \mathbf{x}_3) + Br(\mathbf{x}_2, \mathbf{x}_4) + Br(\mathbf{x}_2, \mathbf{x}_4), \\
& b(e_4) \geq Br(\mathbf{x}_1, \mathbf{x}_4) + Br(\mathbf{x}_2, \mathbf{x}_4) + Br(\mathbf{x}_3, \mathbf{x}_4) + Br(\mathbf{x}_3, \mathbf{x}_5), \\
& b(e_5) \geq Br(\mathbf{x}_1, \mathbf{x}_4) + Br(\mathbf{x}_2, \mathbf{x}_4) + Br(\mathbf{x}_3, \mathbf{x}_4) + Br(\mathbf{x}_1, \mathbf{x}_5) \\
& \qquad + Br(\mathbf{x}_2, \mathbf{x}_5) + Br(\mathbf{x}_3, \mathbf{x}_5), \\
& b(e_6) \geq Br(\mathbf{x}_1, \mathbf{x}_5) + Br(\mathbf{x}_2, \mathbf{x}_5) + Br(\mathbf{x}_3, \mathbf{x}_5) + Br(\mathbf{x}_4, \mathbf{x}_5), \\
& b(e_7) \geq Br(\mathbf{x}_1, \mathbf{x}_4) + Br(\mathbf{x}_2, \mathbf{x}_4) + Br(\mathbf{x}_3, \mathbf{x}_4) + Br(\mathbf{x}_4, \mathbf{x}_5).
\end{aligned}$$

For the general problem, the locations of terminal nodes are given, as are bandwidth capacity requirements between these nodes. We need to optimize the position of Steiner nodes, the bandwidth capacity of each cable edge, and the cable path.

IV. Methodology

Similar to the techniques of [12, 14, 19], the cable network optimization problem can be regarded as an SMT problem. The topology $\mathcal{T}$ is called a *Steiner topology* if the degree of each Steiner node (terminal node) is equal to 3 ($\leq$ 3, respectively) [28]. BUs are at *Steiner nodes* and the CLSs at the *terminal nodes*. Connections between nodes (Steiner and terminal) are edges in the tree. In this paper, the departure from our earlier work is that the capacity of cable between pairs of terminals is considered, so the capacity and cost of each link on the cable network are different. We now consider the problem as an SMT problem with weighted edges.

A. Problem formulation and solutions

For N terminals $\mathbf{x}_1, \mathbf{x}_2, \ldots, \mathbf{x}_N \in \mathbb{M}$ with a given topology $\mathcal{T}$, let $\mathbf{N} = \{1, 2, \ldots, N\}$ be the index set of terminals, $\mathbf{S} = \{N+1, N+2, ..., N+M\}$ the index set of Steiner nodes ($M \leq N-2$), and $\mathbf{V} = \mathbf{N} \cup \mathbf{S}$. Let $\mathbf{E} = \mathbf{E}_1 \cup \mathbf{E}_2$ be the set of all edges, i.e., $\mathcal{T} = (\mathbf{V}, \mathbf{E})$, where $\mathbf{E}_1 = \{(i,j) | i \in \mathbf{N}, j \in \mathbf{S}\}$ and $\mathbf{E}_2 = \{(i,j) | i \in \mathbf{S}, j \in \mathbf{S}\}$. Our problem is to find the coordinates of Steiner nodes: $\mathbf{x}_{N+1}, \mathbf{x}_{N+2}, \ldots, \mathbf{x}_{N+M} \in \mathbb{M}$, the paths $\Gamma = \{\gamma(e) | e \in \mathbf{E}\}$ (i.e., the geodesics corresponding to the edges in $\mathbf{E}$) as well as the specific cable bandwidth level required for the edges, so that the cable network has minimal cost subject to satisfying the bandwidth requirement for each pair of terminal nodes.

We constraint tall terminals and all potential Steiner nodes to be grid nodes $\mathbf{x}_i$ of $\mathbb{M}$, $\mathbf{x}_i \in \mathbb{M}$ (we are only given the coordinates of grid nodes of $\mathbb{M}$ in practice). To accommodate and balance laying costs against risk to the cable, at each grid point $\mathbf{x}$ in $\mathbb{D}$, we let

$$f'(\mathbf{x}, \alpha(\mathbf{x})) = \min_u (h(\mathbf{x}, u) + \alpha \cdot g(\mathbf{x}, u)),$$

where $h(\mathbf{x}, u)$ and $g(\mathbf{x}, u)$ are the laying cost and the repair rate at grid point $\mathbf{x}$, respectively, with cable bandwidth level u. Application of FMM to this cost, produces the optimal path between any pair of grid nodes in $\mathbb{M}$, as described in [14].

Firstly, based on the bandwidth requirement for each path between the specified pair of nodes, we calculate the minimum bandwidth requirement for each cable edge, $B(e_1), ..., B(e_5)$. The per kilometer cable cost of an edge is determined based on the expertise of a cable specialist, and is, say, $\beta(e_1), ..., \beta(e_5)$. Note that, cable bandwidth is fixed within each link. Cables commonly used in the industry typically containing 4, 8, or 16 fibers [7, 29], are ascribed capacities B_4, B_8 and B_{16}, with corresponding costs by C_4, C_8 and C_{16}, respectively. The size of this set of available bandwidths can be varied according to available industry capability. The aim of the problem is to find the optimal positions of BUs, the optimal cable paths connecting two Steiner nodes and Steiner-terminal nodes, and assign appropriate cable bandwidth levels, B_4, B_8 or B_{16}, to each cable edge.

The optimization problem for the total cost $\Psi(\mathcal{T})$, of the physical cable network $\mathcal{T}$, is formulated in Eq. (3).

$$\begin{aligned}&\min_{\mathbf{X},\beta(\cdot),\Gamma} \Psi(\mathbf{x}, \beta(\mathbf{x}), \Gamma)\\ &= \min_{\mathbf{X},\beta(\cdot)} \left(\sum_{j\in\mathbf{S}} \bar{c}_\beta\left(\mathbf{x}_j\right) + \sum_{(i,j)\in\mathbf{E}_2} \min_{\gamma_{ij}} c_\beta\left(\mathbf{x}_i, \mathbf{x}_j\right) \right) + M \cdot c_{BU}\end{aligned} \tag{3}$$

where $\mathbf{x} = \{\mathbf{x}_{N+1}, \mathbf{x}_{N+2}, \ldots, \mathbf{x}_{N+M}\}, \mathbf{x}_{N+j} \in \mathbb{M}$ are coordinates of the Steiner nodes. $\bar{c}_\beta\left(\mathbf{x}_j\right) = \sum_{i\in\mathbf{N},(i,j)\in\mathbf{E}_1} \min_{\gamma_{ij}} c_\beta\left(\mathbf{x}_i, \mathbf{x}_j\right)$ is the sum of the minimum weighted cost from each terminal that is a neighbour of $\mathbf{x}_j$ to $\mathbf{x}_j$ itself, which can be calculated using FMM with the terminal being the source node, while considering the cable bandwidth $\beta(\cdot) \in \{C_4, C_8, C_{16}\}$. Let $\bar{c}_\beta\left(\mathbf{x}_j\right) = 0$ if no terminal is adjacent to the Steiner node $\mathbf{x}_j$, M and c_{BU} are the number and cost of BUs, respectively.

The *skeleton tree* of the topology $\mathcal{T}$ is the subtree $\mathbb{T} = (\mathbf{S}, \mathbf{E}_2)$ composed only of Steiner nodes with the connecting edges, illustrated in Fig. 4.

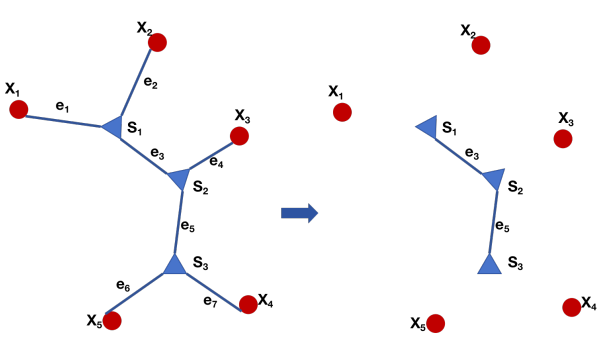

Fig. 4: A Steiner tree and its skeleton tree.

For a tree with a Steiner topology $\mathcal{T}$, we choose an arbitrary Steiner node $\mathbf{s}_r$ as the root of the skeleton tree $\mathbb{T}$, $\mathbf{s}_r \in \mathbb{T}$, and assign to edges of $\mathbb{T}$ an orientation towards the root. Then, $\mathbb{T}$ becomes a directed rooted tree (i.e., anti-arborescence); see Fig. 5(a). For more details on directed rooted trees, see [19]. Nodes of the skeleton tree are ordered so that children of a given node $\mathbf{s}_i$ appear earlier in the list than the parent node (that is, with arrows *from* them to $\mathbf{s}_i$). Such an order is called a *topological order*. Without loss of generality, we can relabel the Steiner nodes as $1, 2, \ldots, M$, where M corresponds to the root of $\mathbb{T}$. We write $\bar{\mathbf{x}}_i = \mathbf{x}_{N+i}, i = 1, 2, ..., M$. Altering the order of Steiner nodes $\mathbf{x}_{N+i} \in \mathbb{M}$ in Eq. (3) does not change the optimization problem, so we have:

$$\begin{aligned}&\min_{\mathbf{x},\beta(\cdot),\Gamma} \Psi(\mathbf{x}, \beta(\mathbf{x}), \Gamma)\\ &\qquad = \min_{\bar{\mathbf{x}}_M, \bar{\mathbf{x}}_{M-1}, \ldots, \bar{\mathbf{x}}_1} \Phi\left(\bar{\mathbf{x}}_M, \bar{\mathbf{x}}_{M-1}, \ldots, \bar{\mathbf{x}}_1\right).\end{aligned} \tag{4}$$

We define $\Phi(\bar{\mathbf{x}}_i) = \bar{c}_\beta(\bar{\mathbf{x}}_i)$ for any leaf i, and

$$\begin{aligned}&\Phi^*\left(\bar{\mathbf{x}}_M, \bar{\mathbf{x}}_{M-1}, \ldots, \bar{\mathbf{x}}_1\right)\\ &= \min_{\bar{\mathbf{x}}_M, \bar{\mathbf{x}}_{M-1}, \ldots, \bar{\mathbf{x}}_1} \Phi\left(\bar{\mathbf{x}}_M, \bar{\mathbf{x}}_{M-1}, \ldots, \bar{\mathbf{x}}_1\right).\end{aligned} \tag{5}$$

Combining this definition with Eq.(3) and (4), we convert the problem to a a dynamic programming (DP) problem:

$$\begin{aligned}&\Phi^*(\bar{\mathbf{x}}_M, \bar{\mathbf{x}}_{M-1}, \ldots, \bar{\mathbf{x}}_1)\\ &\quad = \min_{\bar{\mathbf{x}}_M} \Big[\bar{c}_\beta(\bar{\mathbf{x}}_M) + \sum_{\substack{(j,M)\in E_2\\ j\in C(M)}} \min_{\gamma_{jM}} c_\beta(\bar{\mathbf{x}}_j, \bar{\mathbf{x}}_M)\\ &\qquad + \Phi^*(\bar{\mathbf{x}}_{M-1}, \ldots, \bar{\mathbf{x}}_1) \Big] + M \cdot c_{BU}.\end{aligned} \tag{6}$$

To solve this problem, we construct a new directed acyclic graph (DAG) $\mathbf{G} = (\mathbf{V}', \mathbf{E}')$ based on $\mathbb{T}$, as shown in Fig. 5(b). Each Steiner node $i \in \mathbb{T}$ is associated with a subset $\mathbf{A}_i$ of $\mathbf{V}'$, where $\mathbf{A}_i$ are grid nodes of $\mathbb{M}$ and the weight on each node is $\bar{c}_{ui}(\mathbf{x})$. It follows that $\mathbf{V}' = \cup_{i\in\mathbf{S}}\mathbf{A}_i$; that is, $\mathbf{V}'$ is composed of m copies of the grid nodes of $\mathbb{M}$. For an arc $e = (i, j) \in \mathbf{E}_2$, where $\mathbf{s}_j$ is the parent of $\mathbf{s}_i$, we construct a *complete connection* from $\mathbf{A}_i$ to $\mathbf{A}_j$ for $\mathbf{G}$; that is, an arc $\varepsilon = (p, q)$ from every $\mathbf{x}_p \in \mathbf{A}_i$ to every $\mathbf{x}_q \in \mathbf{A}_j$ in $\mathbf{G}$. The cost of the arc ε is defined as the minimum cost from node $\mathbf{x}_p$ to node $\mathbf{x}_q$, calculated by FMM, i.e., $w(\varepsilon) = w(p, q) = \min c_\beta\left(\mathbf{x}_p, \mathbf{x}_q\right)$. For node $\mathbf{x}_p \in \mathbf{A}_i$, the *minimum cumulative cost* (MCC), ϕ^i_p, is:

$$\phi^i_p = \bar{c}_\beta\left(\mathbf{x}_p\right) + \sum_{j\in C(i)} \min_{q\in \mathrm{A}_j} \left(w\left(\mathbf{x}_q, \mathbf{x}_p\right) + \phi^j_q \right). \tag{7}$$

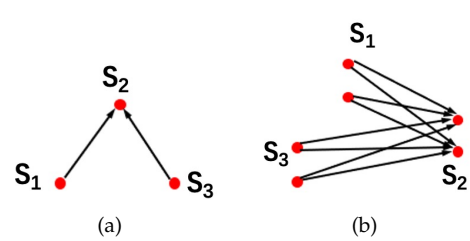

Fig. 5: (a) The skeleton tree with $\mathbf{s}_2$ being the root in Fig. 4. One reordered Steiner node sequence is $\mathbf{s}_1$, $\mathbf{s}_3$, $\mathbf{s}_2$; (b) The DAG corresponding to the Steiner topology and skeleton tree in Fig. 4.

We refer to a previous study [19] that proposes the DAG-Least-Cost-Tree algorithm, which finds the minimum cost tree on a DAG and returns the coordinates of the Steiner nodes. In this paper, we propose a new algorithm called the *weighted edge SMT Algorithm* (WE-SMT Algorithm), which considers cable capacity, cable length, and the number of Steiner nodes to find the minimum total cost tree on a DAG and returns the coordinates of the Steiner nodes. The WE-SMT Algorithm is presented in Algorithm 1. In Algorithm 1, Lines 1-13 calculate the cable cost for the path connecting the leaves of the Steiner node tree with corresponding terminals. Implementation of Eq. (6) is in Lines 14-28. If a leaf node in $\mathbb{T}$ has the same coordinates as a terminal node, then the BU cost $\mathbf{b}_i$ at this location is zero. As in [19], once the iterations reach the root, in Line 32, we choose grid node $\hat{\mathbf{p}}$ (with MCC ϕ_p^M) in $\mathbf{A}_M$. Node $\hat{\mathbf{p}}$ is the physical Steiner node corresponding to the root. To derive the coordinates of the remaining Steiner nodes, we track back on $\mathbf{G}$ starting from $\hat{\mathbf{p}}$. In this way, we find the path γ of the tree with a specific cable bandwidth total cost, and total length. The WE-SMT algorithm, which employs a dynamic programming approach, achieves the optimal solution for a given topology taking into account a specified resolution map and database.

B. Computational complexity analysis of WE-SMT

We assume $|\mathbf{H}|$ grid nodes on the area $\mathbb{M}$ and N terminals to be connected. For a given topology, the complexity analysis is then similar to that in [12,18]. For a given topology with N_b Steiner nodes, the computational complexity of every iteration is $O\left(|\mathbf{H}|^2(\log|\mathbf{H}| + N_b - 1)\right)$ [19]. The cost for each pair of grid nodes on the manifold $\mathbb{M}$ is computed and stored in a database. Therefore, in the worst case, the algorithm requires at least $O\left(|\mathbf{H}|^2\right)$ of memory. We run our algorithm with different data resolutions and display the relationship between the time taken and the resolution in the graph. The experimental results shown in Fig. 11 and Table IV also add to our analysis of algorithm complexity.

V. Numerical Results

In this section, we apply our WE-SMT algorithm to two kinds of realistic scenarios. As in [19], we use bathymetric data from the Global Multi-Resolution Topography synthesis [30]. Our cost function takes account of the trade-off between laying cost and the total number of repairs and the appropriate cable protection at each point in the manifold. The total number of repairs is associated with earthquake-related cable damage risk and human activity-related risk. The cable laying cost is based on the cable bandwidth level and seabed depth. To be realistic, we assume here that the cost of BUs varies between \$1-3 million [31]. The Matlab R2023a code is run on a 4.2 GHz Intel(R) Core(TM) i7-7700K CPU.

Algorithm 1 WE-SMT Algorithm

Input:
The graph $\mathbf{G} = (\mathbf{V}', \mathbf{E}')$, BU cost ($\mathbf{b}_i$) for each BU connecting specified three edges, the cost of each cable edge per kilometer, $\beta(e_1), ..., \beta(e_5)$.

Output:
Coordinates of Steiner nodes $\mathbf{s}_i, i = 1, \ldots, M$, the total cost of the cable network $\Psi(\mathcal{T})$.

1: **for** $i = 1, ..., M$ **do**
2: **for** each node $\mathbf{x}_p \in \mathbf{A}_i$ **do**
3: **if** i is a leaf in $\mathbb{T}$ **then**
4: $\phi_p^i = \bar{c}_\beta\left(\mathbf{x}_p\right) + \mathbf{b}_p$;
5: $\pi\left(\mathbf{x}_p\right) = \mathbf{NIL}$;
6: **else**
7: **for** each child $\mathbf{s}_j$ of $\mathbf{s}_i$ **do**
8: $\pi\left(\mathbf{x}_p, j\right) = \mathrm{NIL}$;
9: **end for**
10: $\phi_p^i = 0$;
11: **end if**
12: **end for**
13: **end for**
14: **for** $i = 1, ..., M$, i is not a leaf **do**
15: **for** each node $\mathbf{x}_p \in \mathbf{A}_i$ **do**
16: **for** each child $\mathbf{s}_j$ of $\mathbf{s}_i$ **do**
17: $\psi = \infty$;
18: **for** each node $\mathbf{x}_q \in \mathbf{A}_j$ **do**
19: $\psi' = \phi_q^j + w\left(\mathbf{x}_q, \mathbf{x}_p\right) + \mathbf{b}_q$
20: **if** $\psi > \psi'$ **then**
21: $\psi = \psi'$;
 $\pi\left(\mathbf{x}_p, j\right) = q$;
22: **end if**
23: **end for**
24: $\phi_p^i = \phi_p^i + \psi$;
25: **end for**
26: $\phi_p^i = \phi_p^i + \bar{c}_\beta\left(\mathbf{x}_p\right)$;
27: **end for**
28: **end for**
29: Let $\hat{p}_M = \arg\min_{\mathbf{x}_p \in \mathbf{A}_M} \phi_p^M$
30: Trace back from $\hat{p}_M$ to leaves via π;
31: **return** $\mathbf{x}_{\hat{p}_1}, \ldots, \mathbf{x}_{\hat{p}_M}$, $\Psi(\mathcal{T})$.

A. The Advantages of the WE-SMT Algorithm over the Non-Bandwidth-aware Algorithm

We present an application of our method to a realistic scenario in the region $\mathbb{D}$, spanning from the northwest corner (45.000°N, 0.000°E) to the southeast corner (36.000°N, 11.000°E). We aim to optimize a cable system that connects the following five locations in this region: Genoa (44.407°N, 8.963°E), Alghero (40.580°N, 8.324°E), Tunis (36.901°N, 7.758°E), Algiers (36.832°N, 3.052°E), and Barcelona (41.399°N, 2.085°E), denoted by A, B, C, D, E, respectively. See Fig. 6(a). The topology of the cable network connecting the five terminals is depicted in Fig. 6(b). The bandwidth for the path between each pair of nodes is shown in Table II.

Based on discussions with an undersea cable ex-

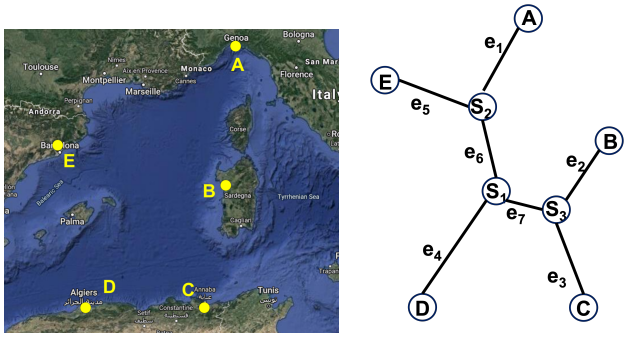

(a) (b)

Fig. 6: (a) Region $\mathbb{D}_1$. Source: Google Earth; (b) A specified topology for five nodes.

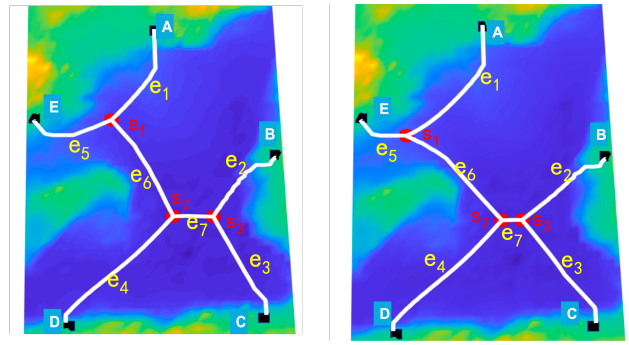

(a) Without bandwidth requirements (b) With bandwidth requirements

Fig. 7: Cable network designs with two different algorithms

pert [29], Table II displays the bandwidth requirements of each edge and the cost per kilometer of cable.

Based on these requirements, we compute the least feasible bandwidth and the cable cost per km for each edge in the tree network, as shown in Table III. Discussions with industry experts have established that the basic bandwidth and cost of cable construction are 50Tbps and $25,000 per km, respectively. These figures, while not exact, serve as a reasonable surrogate for the actual cost, including laying costs. As bandwidth increases, the total cost of cable construction increases as described in Section III.

TABLE II: Bandwidth requirements between pairs of nodes

pairs of nodes	bandwidth	pairs of nodes	bandwidth
(A,B)	10Tbps	(B,D)	20Tbps
(A,C)	20Tbps	(B,E)	10Tbps
(A,D)	10Tbps	(C,D)	30Tbps
(A,E)	10Tbps	(C,E)	20Tbps
(B,C)	30Tbps	(D,E)	10Tbps

TABLE III: Bandwidth requirements of edges.

edge	bandwidth requirement	cable cost per kilometer
e1	50Tbps	$25,000
e2	70Tbps	$27,000
e3	100Tbps	$30,000
e4	70Tbps	$27,000
e5	50Tbps	$25,000
e6	80Tbps	$28,000
e7	110Tbps	$31,000

Leaving aside cable capacity requirements, and assigning all cables the same bandwidth, we can use our earlier algorithm [12] to obtain the network presented in Fig. 7(a).

With this cable configuration, to meet the bandwidth requirements of all paths, capacities of 110Tbps or more are needed, with costs of $31,000 per kilometer, and a total cost of the cable network of $13.312 million.

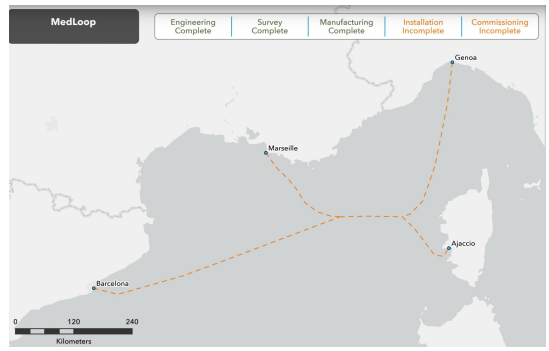

Fig. 8: The Medloop cable network (credit: [1]).

When capacity diversity is used, as shown in Table 1, each edge in the tree network only needs to meet its assigned network bandwidth demand. The resulting optimal network is presented in Fig. 7(b), with a total cost of $9.218 million, representing a 30.75% reduction in cost. In this network, the total length of cable edges e_6 and e_7 have been shortened by 97.75km. As expected, high-capacity cables are shortened to lower the overall cost of the cable network.

B. The Advantages of the WE-SMT Algorithm over the real-world design

In the second example, we evaluate the cost outcomes generated by our algorithm in comparison to a real-world cable system. Specifically, we employ the Medloop cable network situated in the Mediterranean [1] (please see Fig. 8) as our benchmark in this context. This network connects four cities: Marselle (43.29°N, 5.37°E), Genoa (44.41°N, 8.94°E), Barcelona (41.38°N, 2.170°E), Ajaccio (41.91°N, 8.737°E). The total length of this real-world network is 1360km, with a total investment is $34 million. To maintain a fair comparison with the Medloop system, we have omitted the inclusion of weighted costs in this example. The cost of the cable system solely encompasses the construction expenses, without factoring

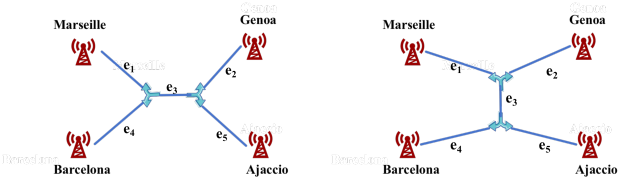

(a) Topology I (b) Topology II

Fig. 9: Two Types of full topologies for tour cities.

in associated risks. This approach is reasonable since there is no apparent risk of earthquakes and fishing in this area. As discussed in Section I, regions characterized by dense populations and well-developed economies exhibit a heightened demand for communication services. To meet the QoS requirements of users, it is important to employ cables with sufficient capacity. In our second example, among the four cities under consideration, both Marseille and Ajaccio are located in France. Marseille is the second-largest city in France and a major economic center. To support commerce, tourism, and cultural exchanges, there's a substantial need for high-bandwidth communication. Ajaccio, with its significant population, serves as an administrative, commercial, and cultural hub in the region. Given the size of their populations and the diversity of economic activities in Marseille and Ajaccio, it becomes evident that these cities have a pronounced demand for increased bandwidth to meet their communication requirements.

To create network connections between the four cities, two full topology options are available, illustrated in Figs. 9(a) and 9(b). The designers of the Medloop cable system chose the first topology for their network design connecting the four cities as shown in [1].

Considering the differences in population among the different cities as discussed above, we assume that the cable path between Marseille and Ajaccio requires a bandwidth of 30Tbps, while the paths between the other pairs of nodes require a bandwidth of 10Tbps. In this four-node network, the bandwidth requirements for the edges of both types of full topologies are identical. According to the bandwidth allocation method outlined in Section III, we have assigned a bandwidth of 50Tbps to edges e_1 and e_5, 30Tbps to edges e_2 and e_4, and 60Tbps to edge e_3. Additionally, the cable costs for the three cable types are \$25,000, \$23,000, and \$26,000 per kilometer, respectively.

We employ the WE-SMT algorithm to optimize the network connecting the four cities in this second example, taking bandwidth into consideration. We compare the WE-SMT cost results with those of the real-world cable system Medloop. The application of WE-SMT was performed on both full topology options separately, and the superior outcome was chosen. The superior result is based on Topology II, which incorporates the introduction of one BU into the cable system, positioned at (43.09°N, 6.78°E). The result is shown in Fig. 10, exhibiting a total length and total cost of 1062km and 28.475 million\$. This represents a 16.25% improvement over the real-world design of the cable system Medloop.

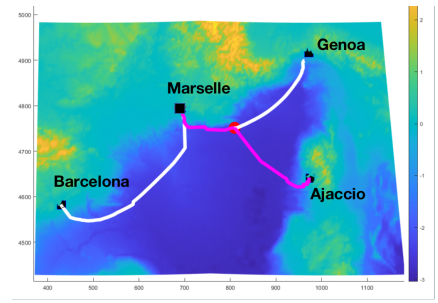

Fig. 10: Results of the WE-SMT Algorithm with Bandwidth Optimization.

C. The Manifestation of WE-SMT Complexity in Runtime

The complexity of the WE-SMT algorithm is reflected in its runtime performance. To demonstrate the complexity of the algorithm, we ran it on maps of seven different resolutions. Among these seven resolutions, the highest has a 1.85km average distance between adjacent grid points, while the six lower resolutions are produced by sampling the highest-resolution map at different spacings. Table IV and Fig. 11 present the runtime and total cost results for WE-SMT at varying map resolutions. As expected, we observe that as the resolution increases, the number of grid nodes ($|N|$) and runtime increases, and the quality of the cable path results improve.

TABLE IV: Performance Comparison of WE-SMT Algorithm at Different Resolutions.

Resolution (km)	Total number of grid nodes	Total cost (million \$)	Runtime (s)
18.5	$1.26 * 10^3$	33.042	0.091
13.89	$2.22 * 10^3$	32.834	0.301
9.25	$6.0 * 10^3$	32.718	0.613
4.62	$1.96 * 10^4$	31.382	0.901
3.70	$3.05 * 10^4$	29.103	1.271
2.77	$5.41 * 10^4$	28.902	2.453
1.85	$1.22 * 10^5$	28.218	6.902

VI. Conclusion

Undersea fiber optic cables are a critical component of the global telecommunications infrastructure, responsible for transmitting vast amounts of data across oceans, and connecting people and businesses around the world. Higher numbers and quality of optical fibers in a cable lead to higher costs. Construction of an undersea cable system requires consideration of the appropriate bandwidth capacity to meet network requirements while minimizing costs. We have formulated this optimization problem as a weighted edges Steiner minimum tree problem, taking into account the bandwidth capacity of each edge, and have proposed the WE-SMT algorithm to solve it. This algorithm optimizes the network by

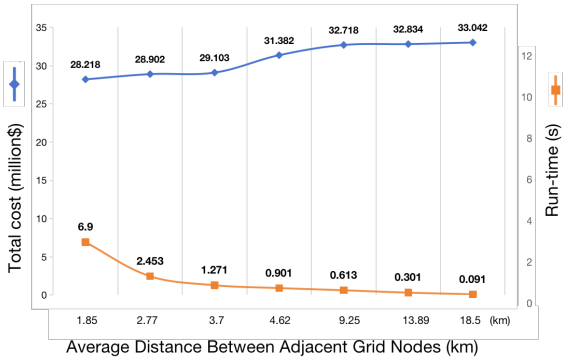

Fig. 11: Performance Comparison of WE-SMT Algorithm at Different Resolutions

optimizing the locations of Steiner nodes, the bandwidth capacity of each cable edge, and the cable path for given terminal node locations and bandwidth capacity requirements.

Overall, this paper represents a significant advance in undersea cable system optimization research by developing a new approach and algorithm that can effectively optimize the positions of Steiner nodes, bandwidth capacity, and cable paths while taking into account the requirements of real-world scenarios.

Acknowledgment

The authors wish to thank Andrew Hankins for highlighting the importance of including cable capacity considerations in the design of cable systems. This provided the motivation for the work presented in this paper.

References

[1] "Submarine telecoms industry report," Submarine Telecoms Forum, Inc., Sterling, Virginia, USA, Tech. Rep., Oct. 2021 (accessed on 20 Dec., 2023). [Online]. Available: https://subtelforum.com/products/submarine-telecoms-industry-report/

[2] L. D. Garrett, "Design of global submarine networks," *Journal of Optical Communications and Networking*, vol. 10, no. 2, pp. A185–A195, 2018.

[3] L. Carter, *Submarine cables and the oceans: connecting the world*. UNEP/Earthprint, 2009, no. 31.

[4] C. R. Service, "Undersea Telecommunication Cables: Technology Overview and Issues for Congress," Sep. 2022.

[5] J. Kim, "Fiber Optics: What is it? and How Does it Work?" Feb. 2023 (accessed on Mar. 2023). [Online]. Available: https://dgtlinfra.com/fiber-optics/

[6] H. T. *et al.*, "Past, current and future technologies for optical submarine cables," *Proc. 2019 IEEE/ACM Workshop on Photonics-Optics Technology Oriented Networking, Information and Computing Systems*, vol. 248, pp. 36–42, Nov. 2019.

[7] TeleGeography, "Submarine Cable Frequently Asked Questions," 2021 (accessed on Mar. 2023). [Online]. Available: https://www2.telegeography.com/submarine-cable-faqs-frequently-asked-questions

[8] J. Kim, "Submarine Cables: the Invisible Fiber Link Enabling the Internet," May 2022 (accessed on Nov. 2023). [Online]. Available: https://dgtlinfra.com/submarine-cables-fiber-link-internet/

[9] X. ZHENG, J. TAN, S. Jiang, and C. Wang, "Analysis on the requirements of future data network," *Telecommunications Science*, vol. 35, no. 8, pp. 16–25, 2019.

[10] U. One, "Enhancing Public Services with Fiber Construction," Aug. 2023. [Online]. Available: https://utilitiesone.com/enhancing-public-services-with-fiber-construction

[11] T. Wang, X. Wang, Z. Wang, C. Guo, W. Moran, and M. Zukerman, "Optimal tree topology for a submarine cable network with constrained internodal latency," *Journal of Lightwave Technology*, vol. 39, no. 9, pp. 2673–2683, 2021.

[12] T. Wang, Z. Wang, B. Moran, and M. Zukerman, "Submarine cable network design for regional connectivity," *IEEE/ACM Transactions on Networking*, 2022.

[13] T. Wang, X. Wang, Z. Wang, C. Guo, W. Moran, and M. Zukerman, "Latency-aware optimization of submarine communication cable systems with trunk-and-branch topologies," *Journal of Lightwave Technology*, vol. 40, no. 17, pp. 5825–5841, 2022.

[14] Z. Wang, Q. Wang, M. Zukerman, J. Guo, Y. Wang, G. Wang, J. Yang, and B. Moran, "Multiobjective path optimization for critical infrastructure links with consideration to seismic resilience," *Computer-Aided Civil and Infrastructure Engineering*, vol. 32, no. 10, pp. 836–855, 2017.

[15] X. Wang, Z. Wang, E. Tahchi, and M. Zukerman, "Submarine cable path planning based on weight selection of design considerations," *IEEE Access*, vol. 9, pp. 123 847–123 860, 2021.

[16] S. Blaise and B. Spinewine, "Efficient curvature-constrained least cost route optimization on parallel architectures," *Engineering with Computers*, vol. 38, no. Suppl 3, pp. 2041–2057, 2022.

[17] J. A. Sethian, *Level set methods and fast marching methods: evolving interfaces in computational geometry, fluid mechanics, computer vision, and materials science 2nd Edition*. Cambridge University Press, August 1999.

[18] J. Yang and F. Stern, "A highly scalable massively parallel fast marching method for the eikonal equation," *Journal of computational physics*, vol. 332, pp. 333–362, 2017.

[19] Z. Wang, Q. Wang, B. Moran, and M. Zukerman, "Optimal submarine cable path planning and trunk-and-branch tree network topology design," *IEEE/ACM Transactions on Networking*, vol. 28, no. 4, pp. 1562–1572, Aug. 2020.

[20] A. Ivanov and A. Tuzhilin, "Analytic deformations of minimal networks," *Journal of Mathematical Sci-*

ences, vol. 248, pp. 621–635, 2020.

[21] A. O. Ivanov and A. A. Tuzhilin, *Minimal Networks: The Steiner Problem and Its Generalizations*. CRC press, 1994.

[22] J. D. Downie, X. Liang, and S. Makovejs, "Assessing capacity and cost/capacity of 4-core multicore fibers against single core fibers in submarine cable systems," *Journal of Lightwave Technology*, vol. 38, no. 11, pp. 3015–3022, 2020.

[23] ——, "Examining the case for multicore fibers in submarine cable systems based on fiber count limits," *IEEE Journal of Selected Topics in Quantum Electronics*, vol. 26, no. 4, pp. 1–9, 2020.

[24] C. Cao, M. Zukerman, W. Wu, J. H. Manton, and B. Moran, "Survivable topology design of submarine networks," *Journal of lightwave technology*, vol. 31, no. 5, pp. 715–730, 2013.

[25] J. Zhang, E. Modiano, and D. Hay, "Enhancing network robustness via shielding," *IEEE/ACM Transactions on Networking*, vol. 25, no. 4, pp. 2209–2222, 2017.

[26] S. Neumayer, G. Zussman, R. Cohen, and E. Modiano, "Assessing the vulnerability of the fiber infrastructure to disasters," *IEEE/ACM Transactions on Networking*, vol. 19, no. 6, pp. 1610–1623, 2011.

[27] MAKAI OCEAN ENGINEERING, "The Future of Ocean Innovation," 2015. [Online]. Available: https://www.makai.com/cable-software/

[28] M. Fampa and K. M. Anstreicher, "An improved algorithm for computing Steiner minimal trees in Euclidean d-space," *Discrete Optimization*, vol. 5, no. 2, pp. 530–540, 2008.

[29] E. Tahchi, private communication, October 2016.

[30] "Global Multi-Resolution Topography Data Synthesis," Oct. 2019.

[31] R. Hale, private communication, Mar. 2021.